CHAPTER 4

EXPERIMENTAL RESULTS

4.1 Test Conditions

Three different water injection pressures and four different volumetric ratios were chosen as the desired conditions for the experiments. The water injection pressure is varied from 2 bar (g) to 4 bar (g). The volume of the injected water is varied from 100 cc to 400 cc, while the liquid nitrogen is kept constant at 2000 cc. This gives the volumetric ratio of 0.05 to 0.20. The desired test conditions are shown in Table 4.1.

Table 4.1 Test conditions with 2000-cc liquid nitrogen

Experiment No.	Water injection pressure, bar (g)	Injected water cc
#1	2	100
#2	2	200
#3	2	300
#4	2	400
#5	3	100
#6	3	200
#7	3	300
#8	3	400
#9	4	100
#10	4	200
#11	4	300
#12	4	400

4.2 Experimental Results

In most tests, the water in the pressurized bottle was totally injected into the interaction chamber. The experiments in which some of the water was left in the bottle were the #3 and #4 tests conducted with the injection pressure of 2 bars and with the water/liquid nitrogen volume ratio of 0.15 and 0.20. Thus, all experimental results are shown in this dissertation except the results from the test #3 and #4.

The pressure profiles obtained with the pressure transducers from the experiments are shown in Fig. 4.1, 4.2 and 4.3. In each figure, the vertical axis of each graph give the gauge pressure in the unit of bar while the horizontal axis was for the time of observation, where the time zero was the time at which the injection of the water was initiated, in the unit of milliseconds.

In each graph, four pressure profiles are presented. In general, the top most profile is for the pressure obtained by the transducer PT1 during the interaction. The profile that normally lies just lower to the first one was obtained with the transducer PT2 in the same event. The other two profiles are those lied at the lower part of each graph and are virtually identical. Those profiles are obtained from the experiments in which no liquid nitrogen is filled into the chamber. Therefore, each profile that is obtained is actually due to the pressure from the bottle. This is done to confirm that the profiles obtained during the experiments with the water injection are really the results from the interaction between the water and the liquid nitrogen.

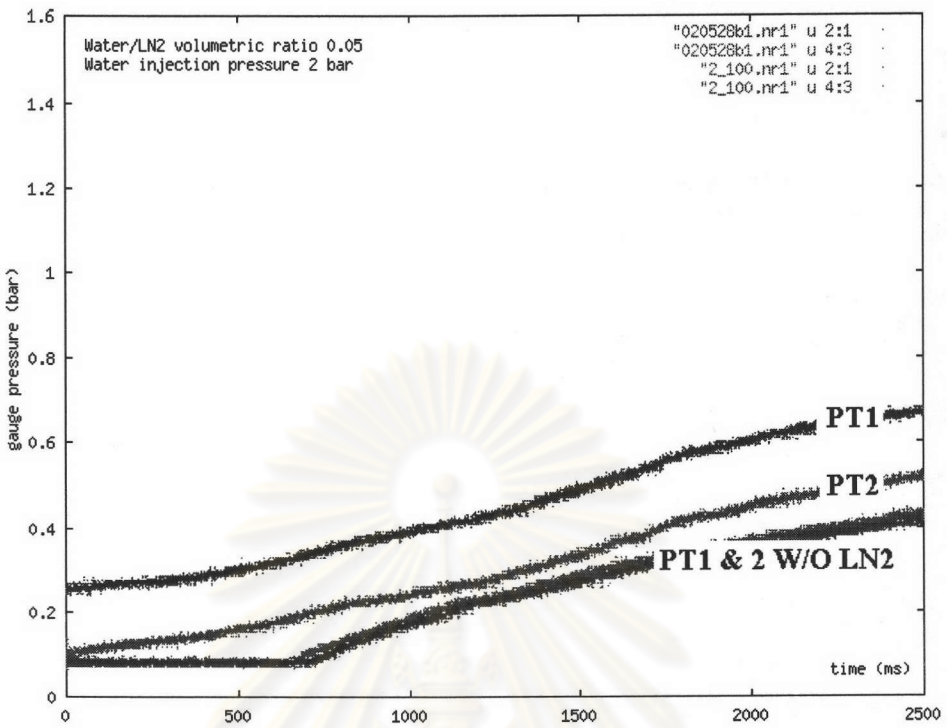

(a) volumetric ratio 0.05

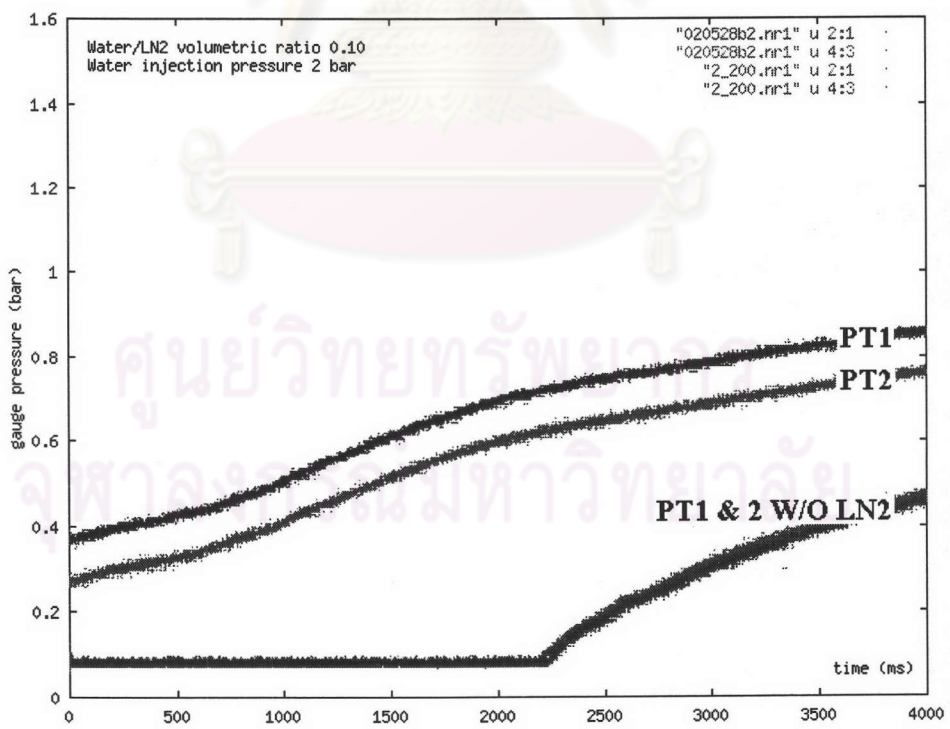

(b) volumetric ratio 0.10

Fig. 4.1 The pressure profiles obtained from the experiments with the injection pressure of 2 bars

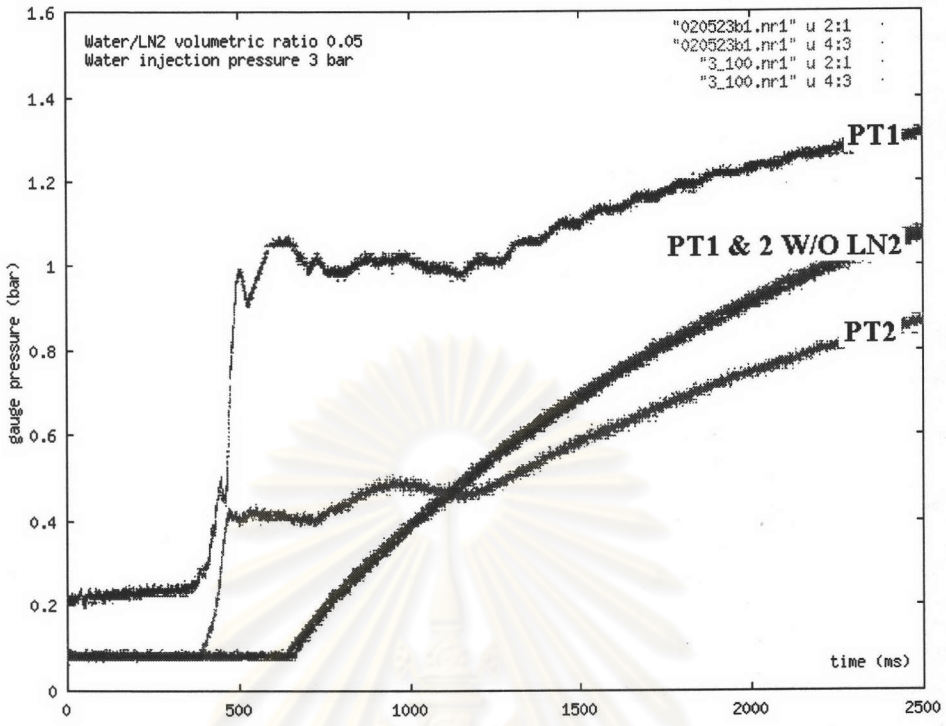

(a) volumetric ratio 0.05

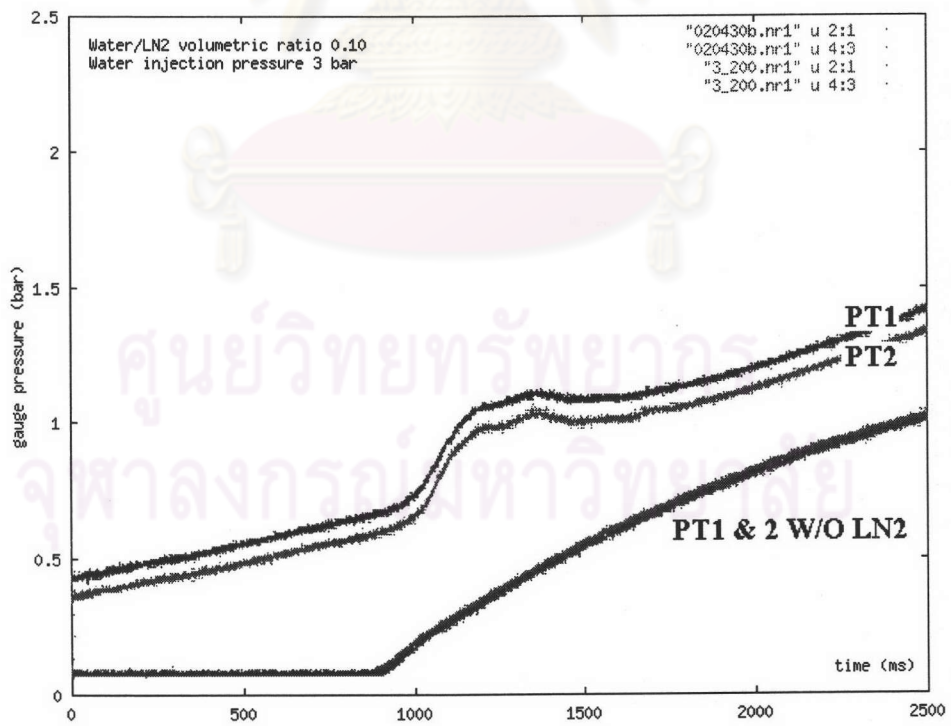

(b) volumetric ratio 0.10

Fig. 4.2 The pressure profiles obtained from the experiments with the injection pressure of 3 bars

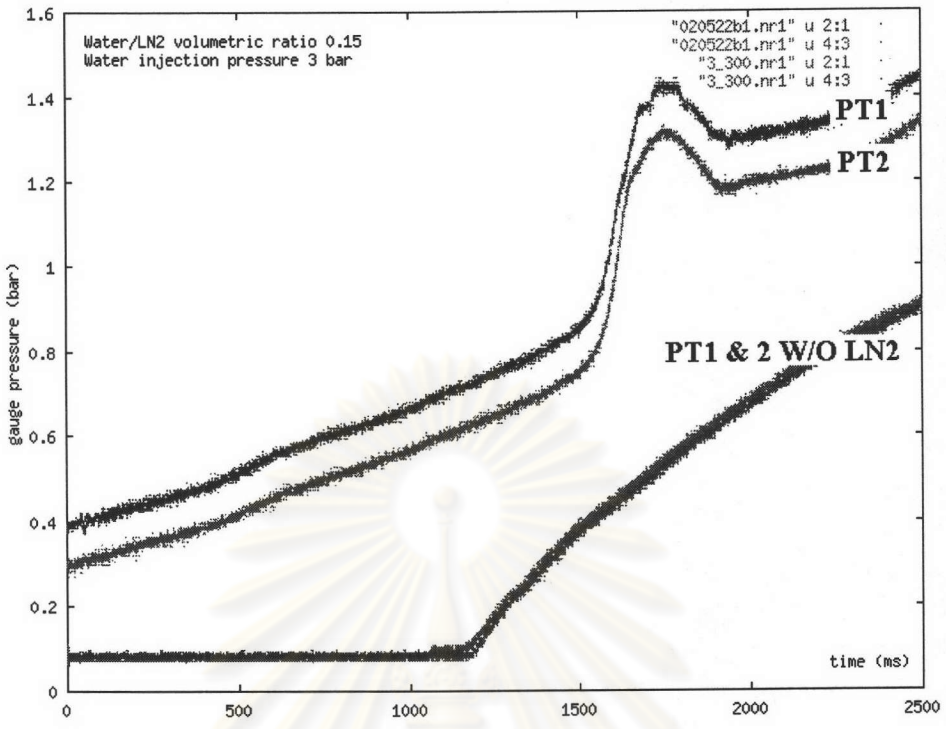

(c) volumetric ratio 0.15

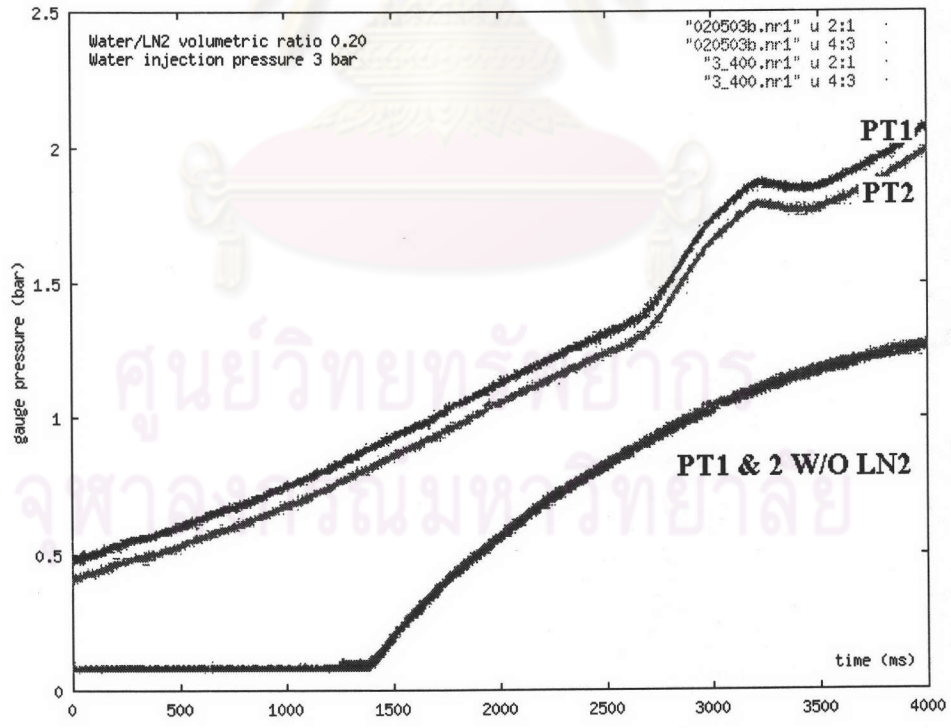

(d) volumetric ratio 0.20

Fig. 4.2 (cont.) The pressure profiles obtained from the experiments with the injection pressure of 3 bars

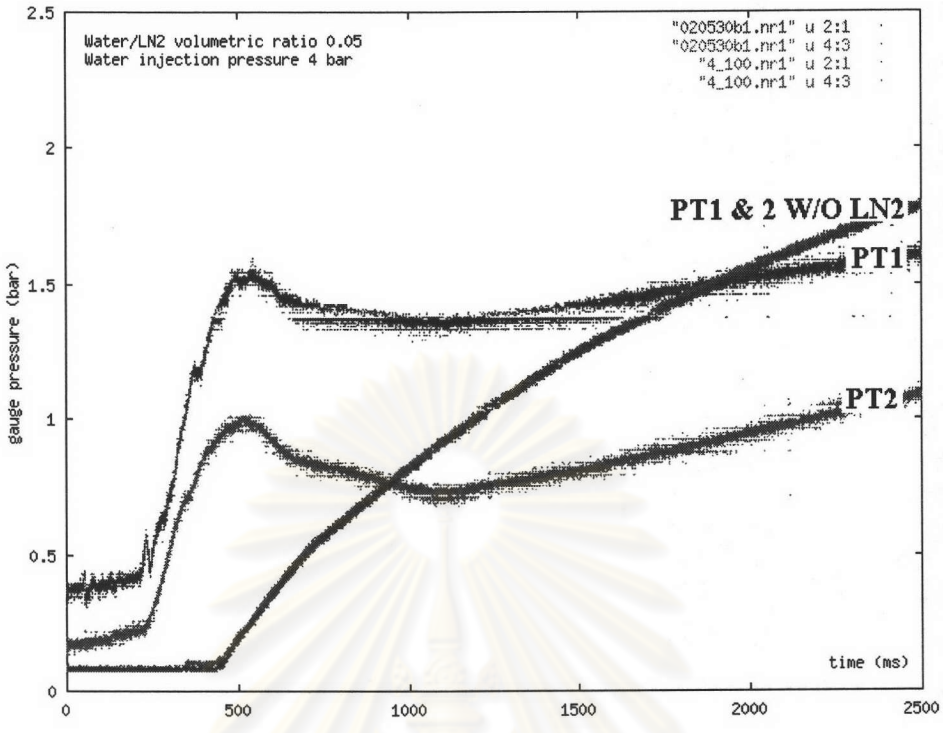

(a) volumetric ratio 0.05

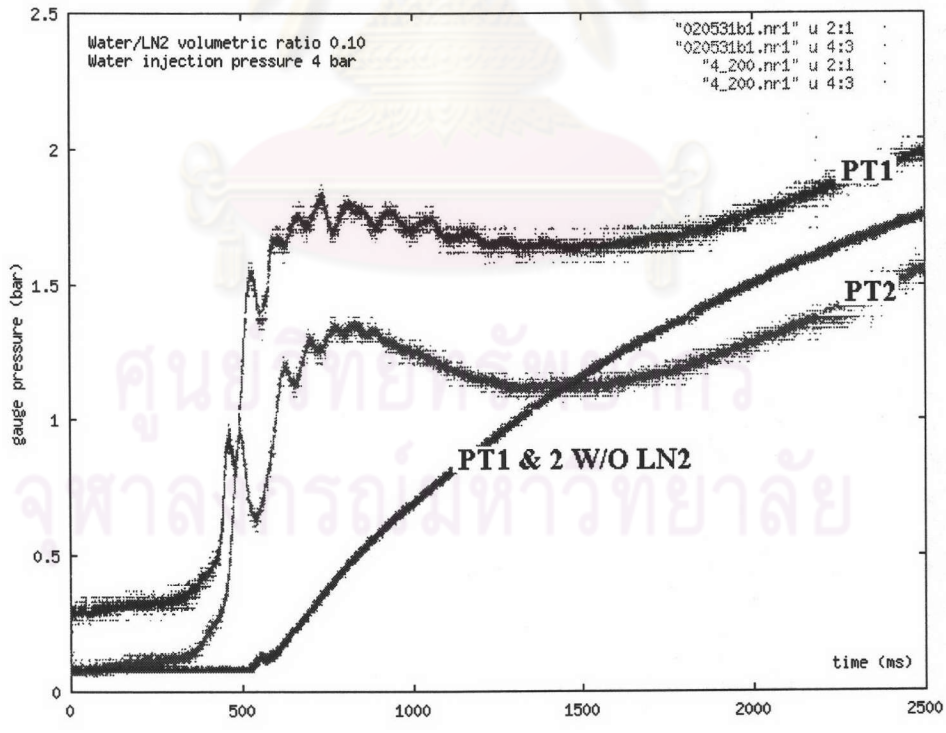

(b) volumetric ratio 0.10

Fig. 4.3 The pressure profiles obtained from the experiments with the injection pressure of 4 bars

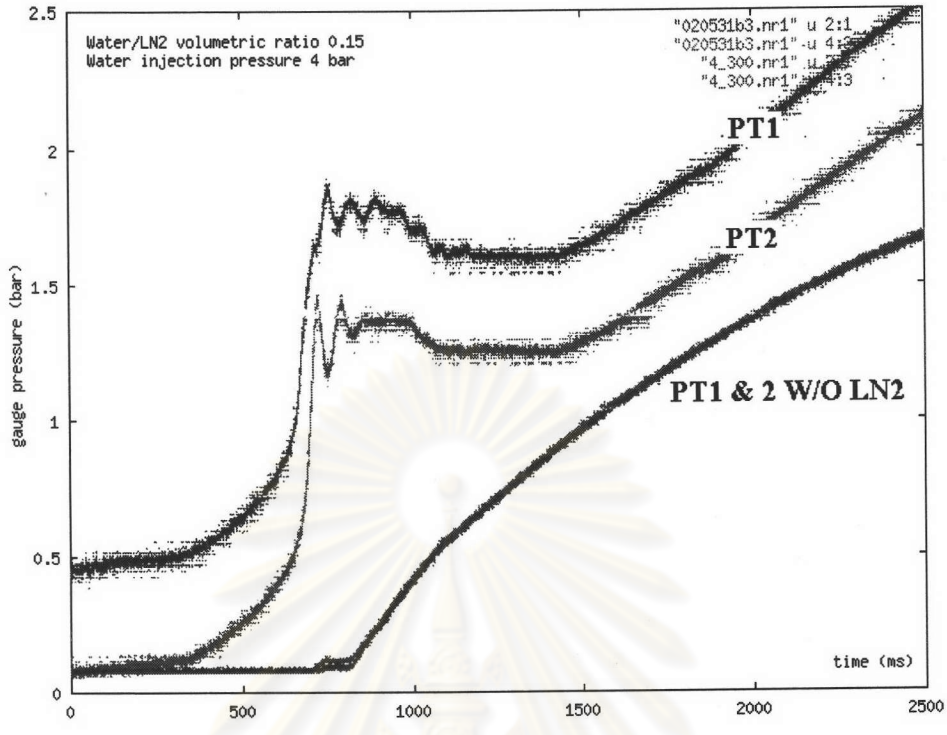

(c) volumetric ratio 0.15

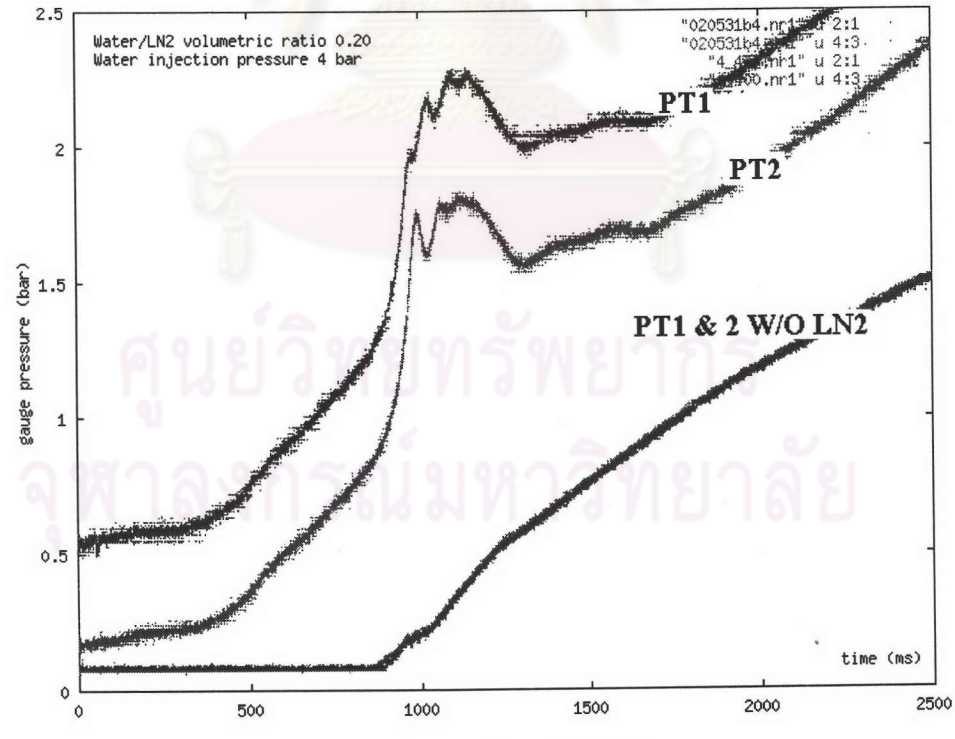

(d) volumetric ratio 0.20

Fig. 4.3 (cont.) The pressure profiles obtained from the experiments with the injection pressure of 4 bars

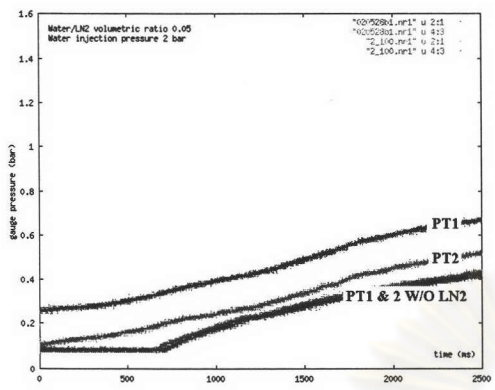

(a)

(b)

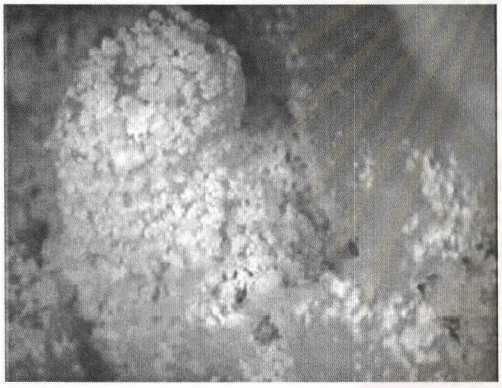

(c)

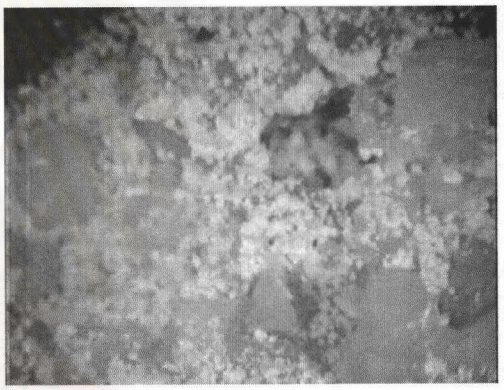

(d)

Fig. 4.4 Pressure profiles (a) and its ice debris (b), (c), and (d) from test #1 with injection pressure of 2 bar and volumetric ratio 0.05

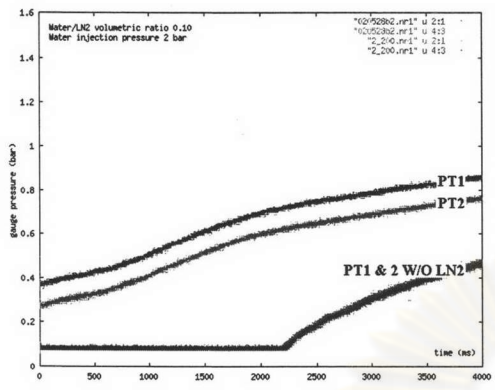

(a)

(b)

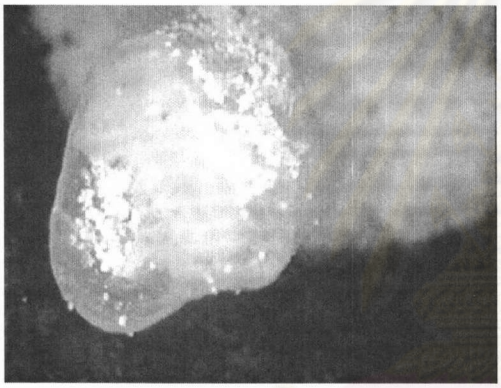

(c)

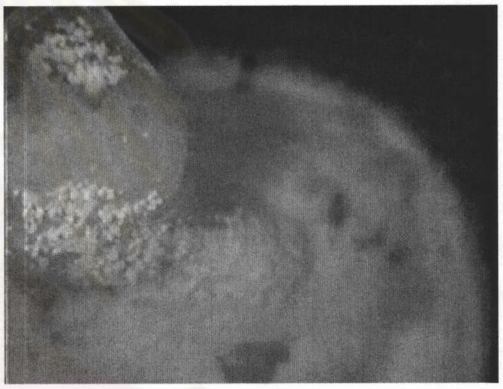

(d)

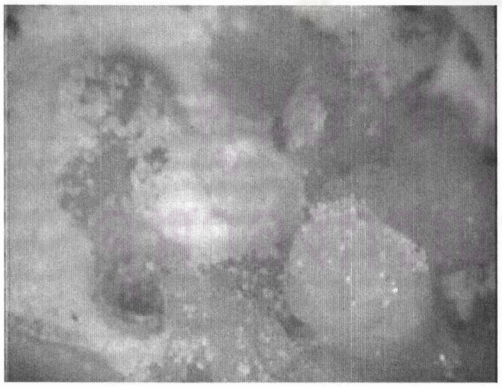

(e)

(f)

Fig. 4.5 Pressure profiles (a) and its ice debris (b), (c), (d), (e), and (f) from test #2 with injection pressure of 2 bar and volumetric ratio 0.10

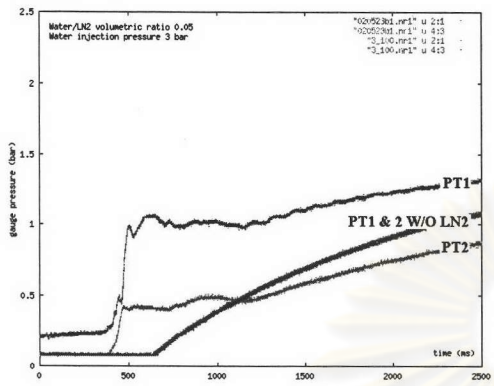

(a)

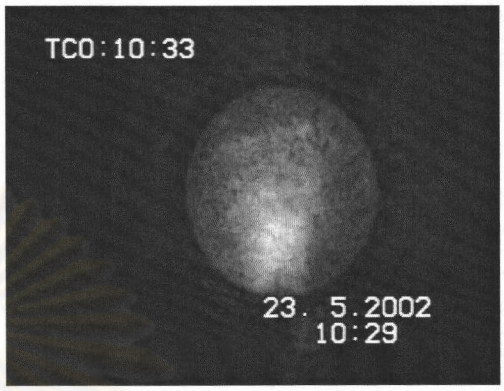

(b)

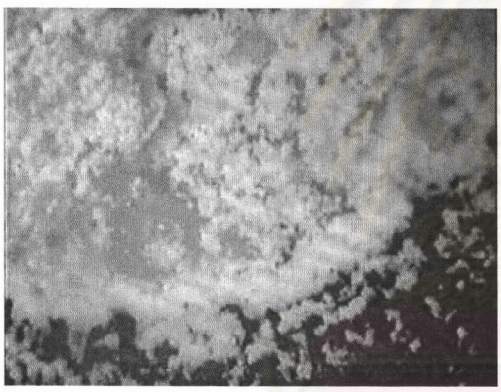

(c)

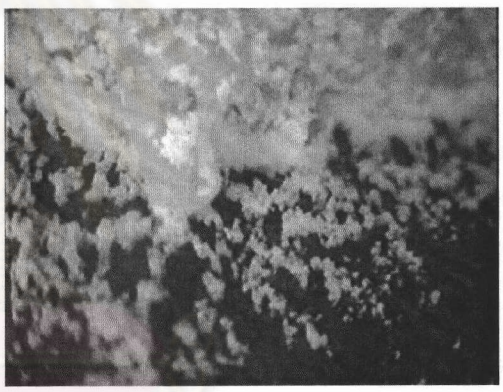

(d)

(e)

(f)

Fig. 4.6 Pressure profiles (a) and its ice debris (b), (c), (d), (e), and (f) from test #5 with injection pressure of 3 bar and volumetric ratio 0.05

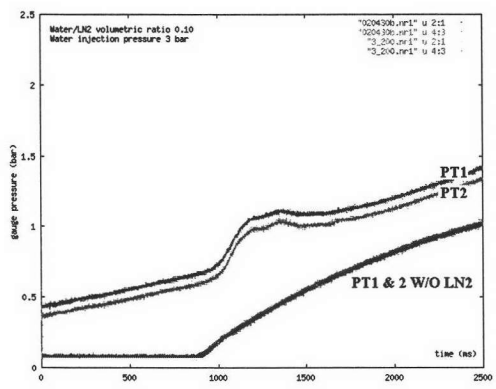

(a)

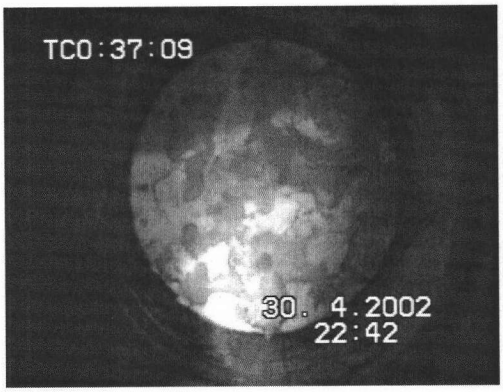

(b)

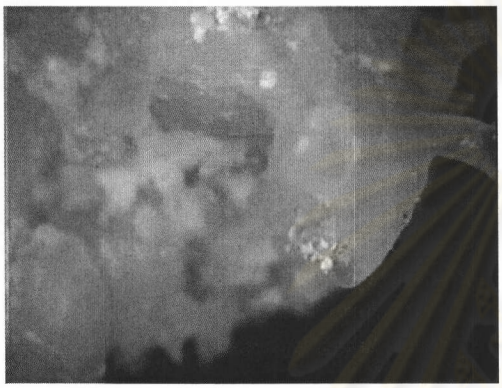

(c)

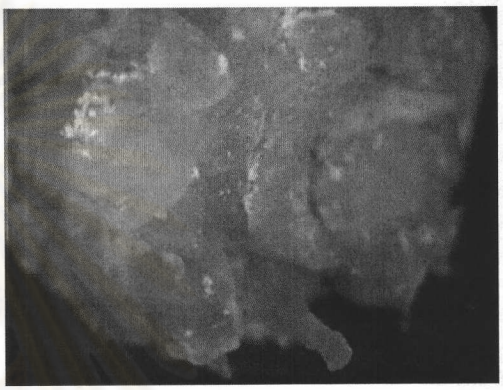

(d)

(e)

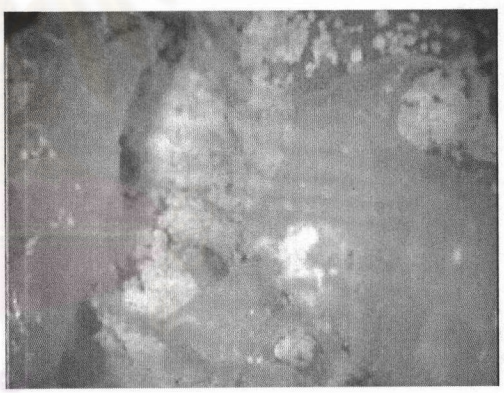

(f)

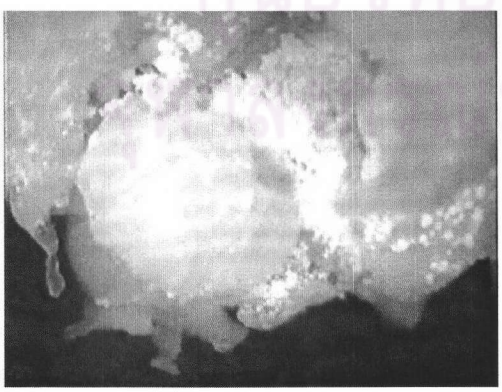

(g)

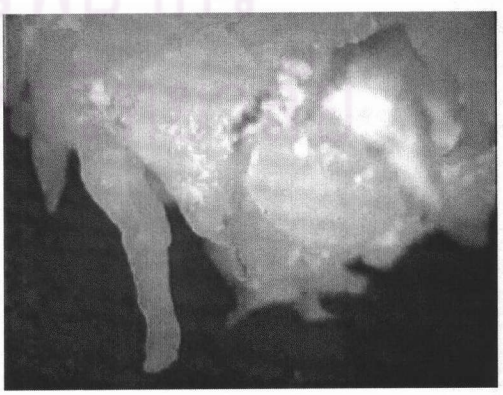

(h)

Fig. 4.7 Pressure profiles (a) and its ice debris (b), (c), (d), (e), (f), (g), and (h) from test #6 with injection pressure of 3 bar and volumetric ratio 0.10

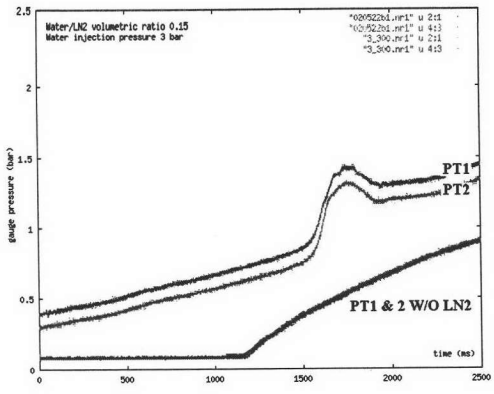

(a)

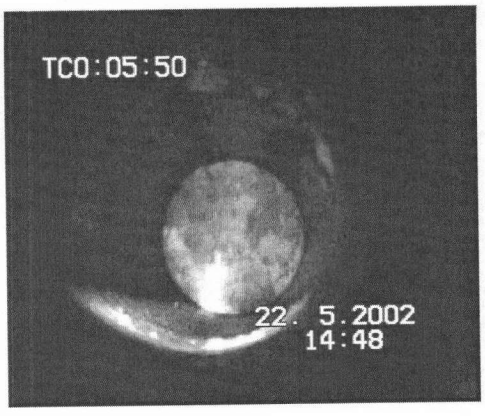

(b)

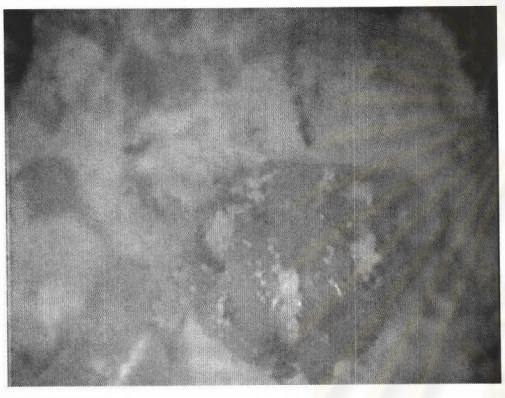

(c)

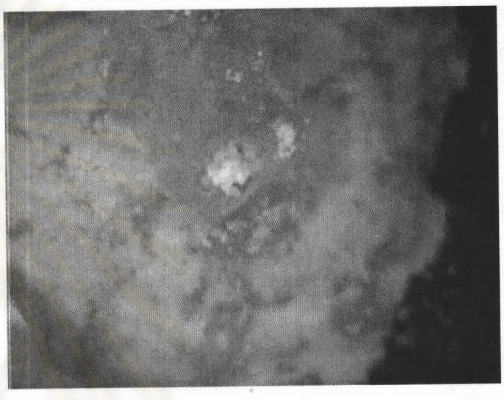

(d)

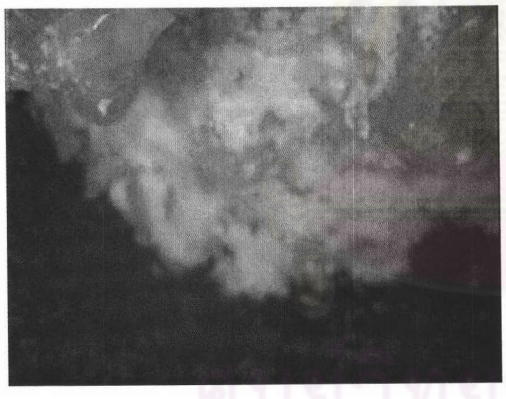

(e)

(f)

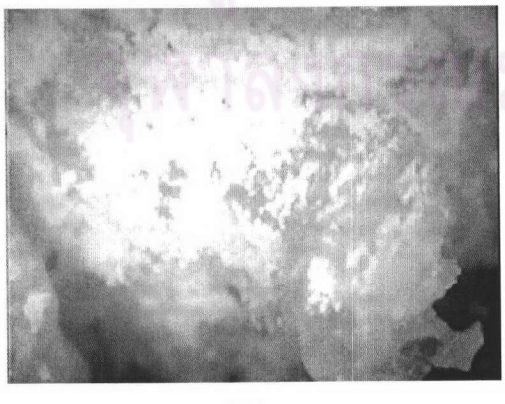

(g)

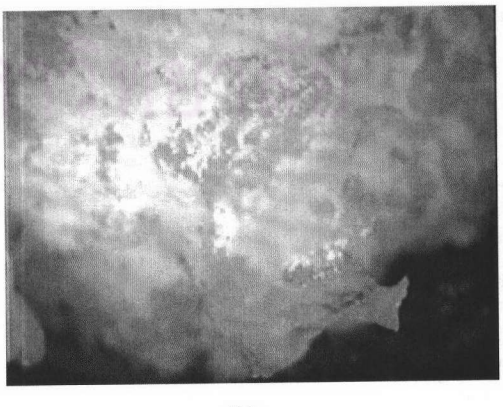

(h)

Fig. 4.8 Pressure profiles (a) and its ice debris (b), (c), (d), (e), (f), (g), and (h) from test #7 with injection pressure of 3 bar and volumetric ratio 0.15

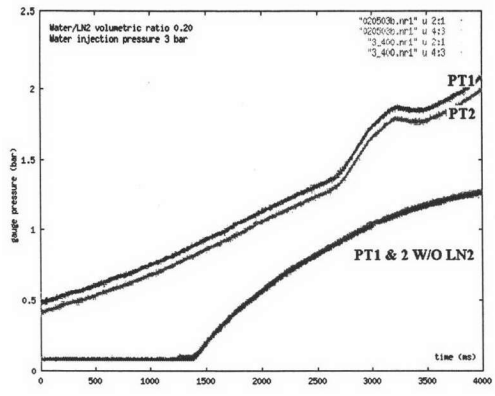

(a)

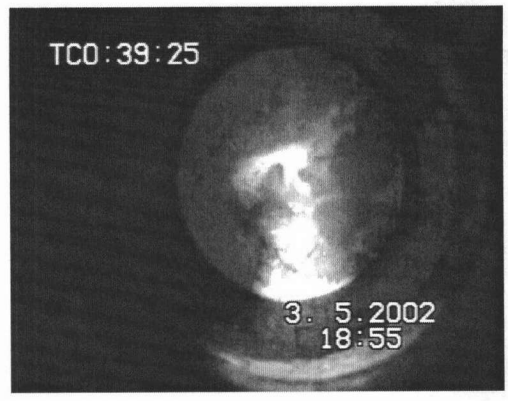

(b)

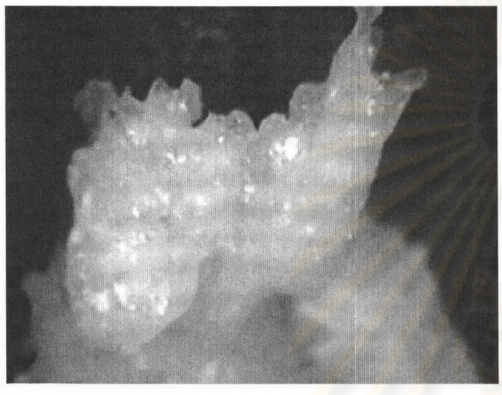

(c)

(d)

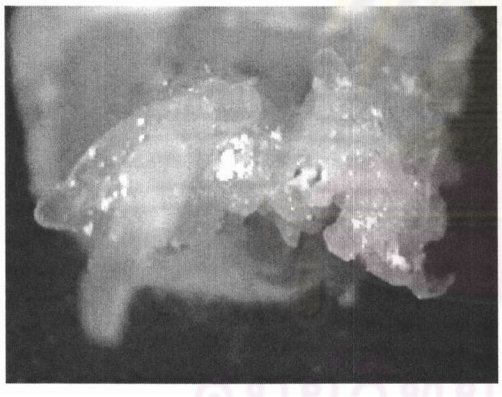

(e)

(f)

(g)

(h)

Fig. 4.9 Pressure profiles (a) and its ice debris (b), (c), (d), (e), (f), (g), and (h) from test #8 with injection pressure of 3 bar and volumetric ratio 0.20

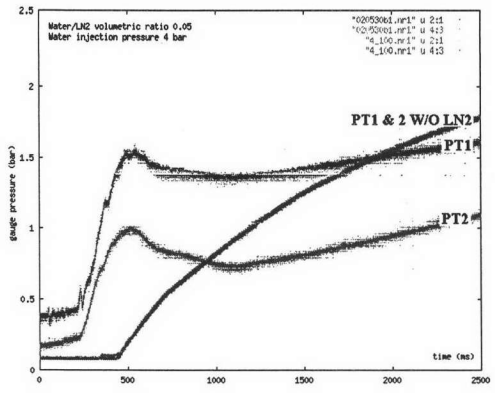

(a)

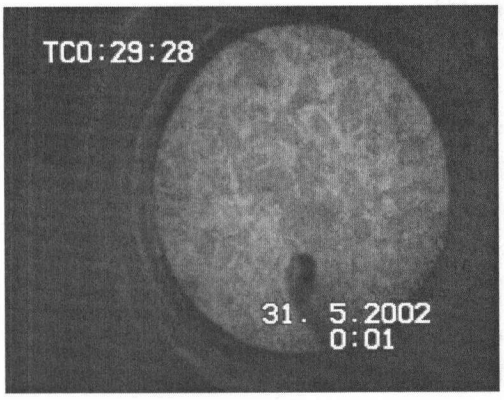

(b)

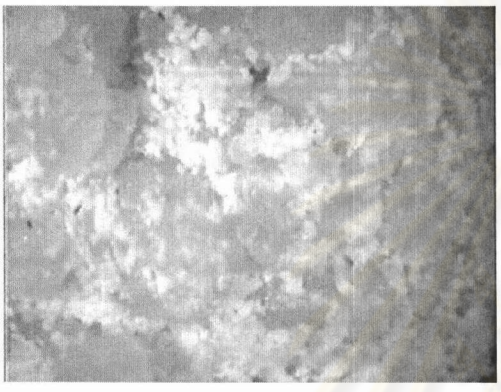

(c)

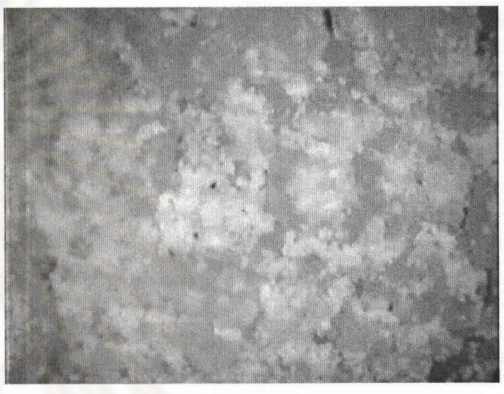

(d)

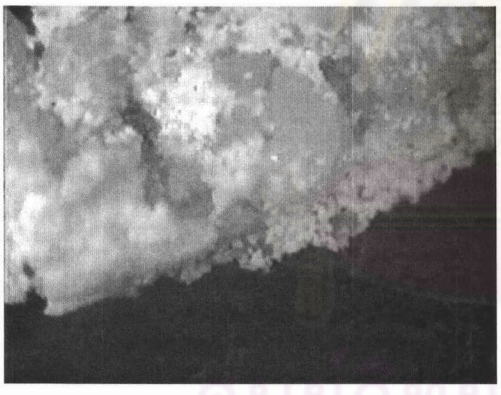

(e)

(f)

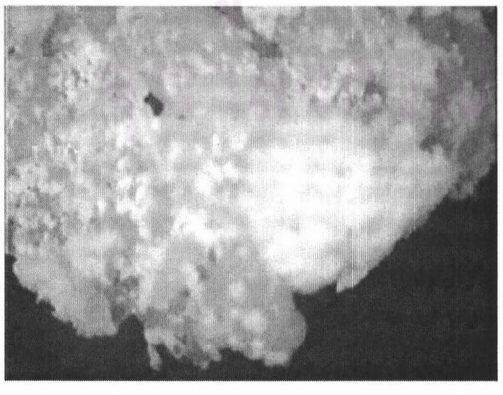

(g)

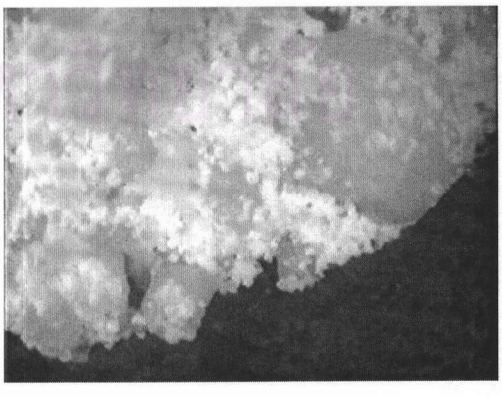

(h)

Fig. 4.10 Pressure profiles (a) and its ice debris (b), (c), (d), (e), (f), (g), and (h) from test #9 with injection pressure of 4 bar and volumetric ratio 0.05

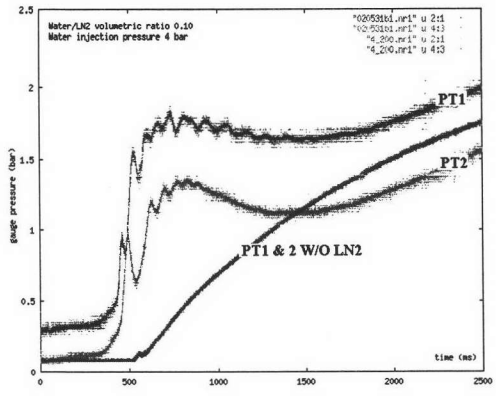

(a)

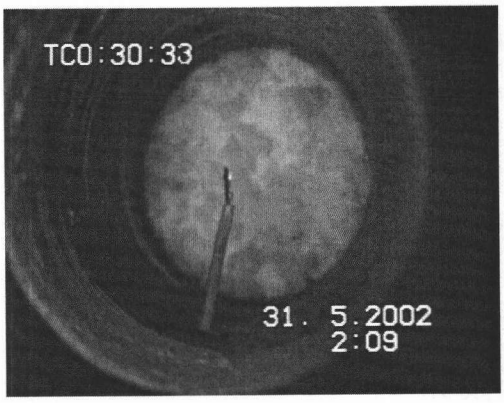

(b)

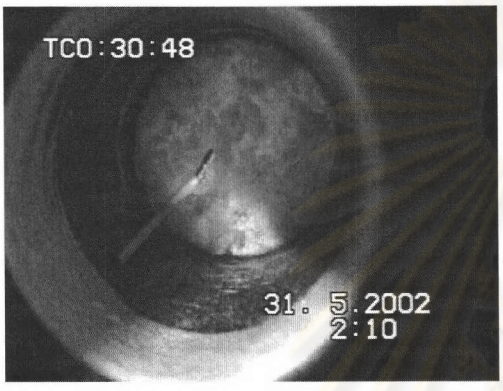

(c)

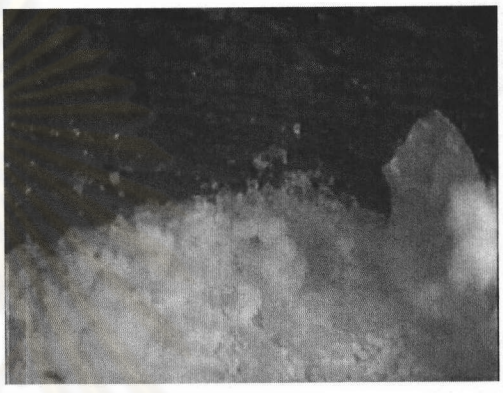

(d)

(e)

(f)

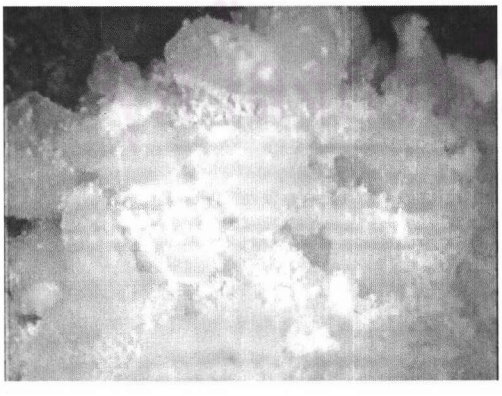

(g)

Fig. 4.11 Pressure profiles (a) and its ice debris (b), (c), (d), (e), (f), and (g) from test #10 with injection pressure of 4 bar and volumetric ratio 0.10

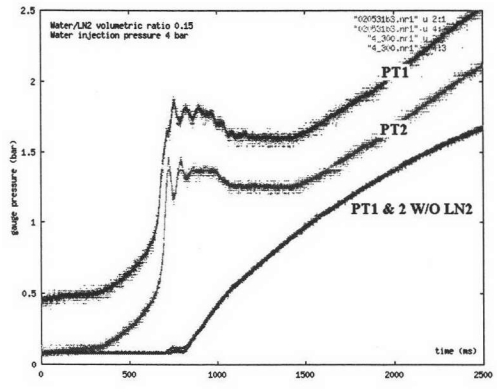

(a)

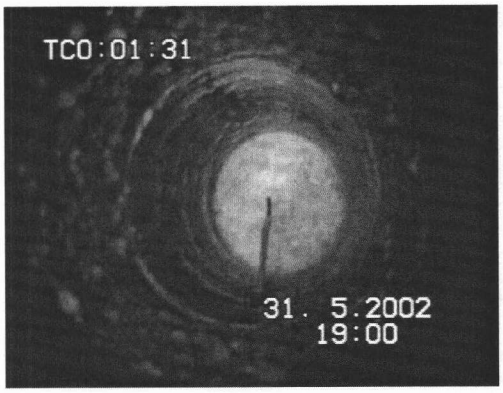

(b)

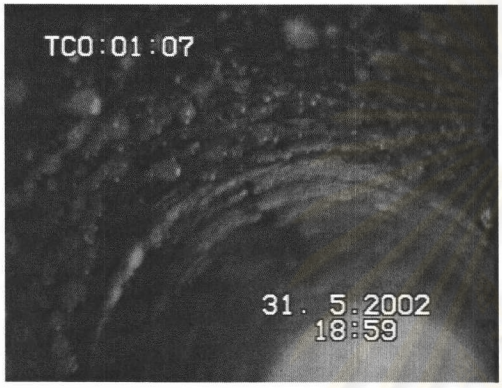

(c)

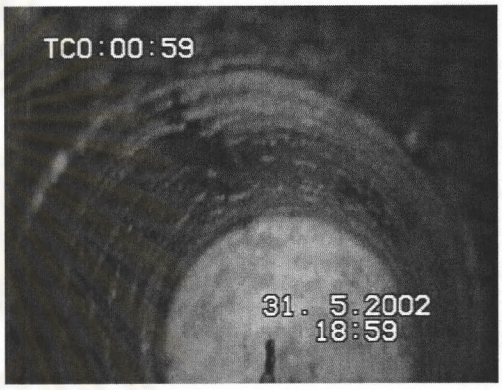

(d)

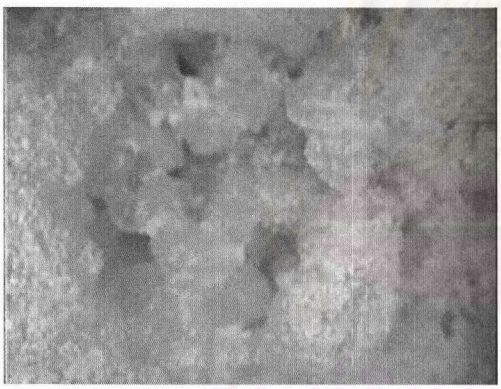

(e)

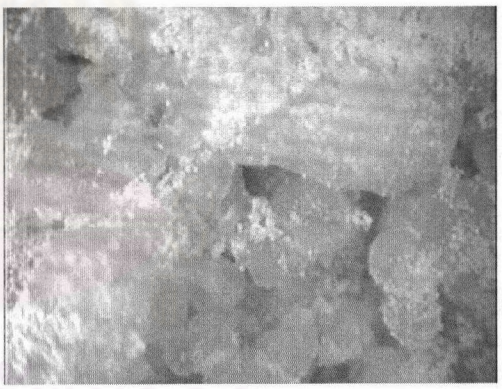

(f)

(g)

Fig. 4.12 Pressure profiles (a) and its ice debris (b), (c), (d), (e), (f), and (g) from test #11 with injection pressure of 4 bar and volumetric ratio 0.15

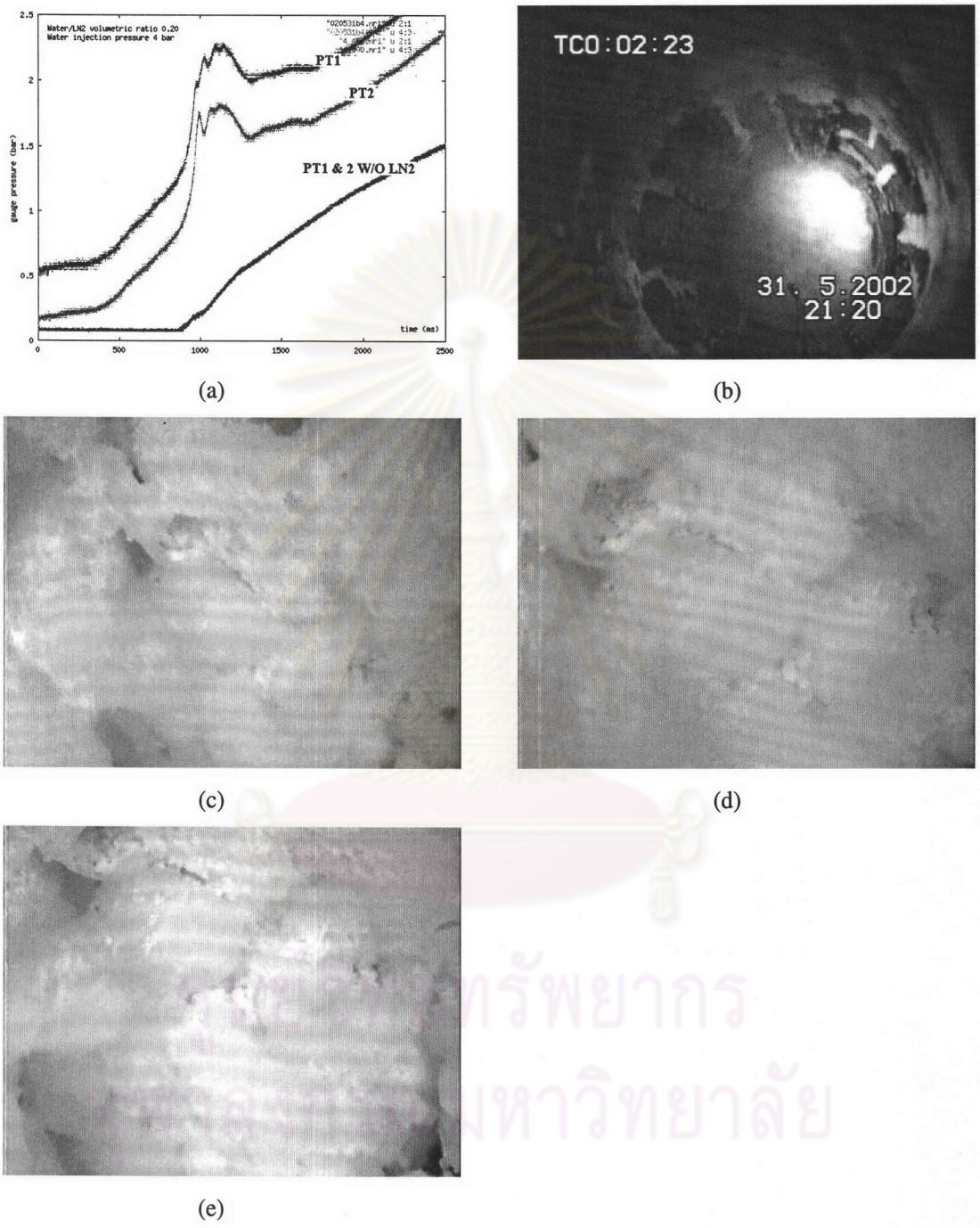

(a) (b)

(c) (d)

(e)

Fig. 4.13 Pressure profiles (a) and its ice debris (b), (c), (d), and (e)
from test #12 with injection pressure of 4 bar and volumetric ratio 0.20

4.3 Analyses

4.3.1 Pressure Profiles

From the pressure profiles as obtained without the liquid nitrogen, both transducers gave virtually the same results. This was expected since there was no interaction. In effect, this confirmed that both transducers were working correctly. When the full experiments were conducted, i.e., the water and the liquid nitrogen were used; the pressure profiles were clearly separated even at the beginning of the observation. This was because of the heating of the liquid nitrogen at the wall of the chamber. Since the vaporized nitrogen was much denser than the normal air that filled the upper part of the chamber, the vaporized nitrogen would diffuse at the very slow rate to the upper part of the chamber and, thus, caused the pressure at the lower part of the chamber to be higher. The higher pressure obtained with PT1 at the beginning of the observation confirmed this explanation.

The results obtained from the full experiments were summarized as given in Table 2. In some experiments, the pressure spikes could be observed. On the other hand, only the pressurization process was observed in the other experiments. It must be stated that, in identifying the pressure spike, the pressure should have been increasing at the relatively very high rate and should have occurred early in the experiment when the water injection was still in progress. It was observed that the pressure spikes were rarely observed in the experiments where the low pressure was used to inject the water.

As a side note, it was observed that in each of the experiments where the pressure spikes were observed, the installation was found visibly shaking, while the audible sound from inside the chamber could be heard. This suggested that the interaction in each of these experiments must be quite violent.

Based on the existence of the pressure spikes in the experiments, a diagram for the possible "Interaction Zone" is created. This diagram is shown in Fig. 4.14. The

diagram shows the water injection pressure as its vertical axis and the water/liquid nitrogen volumetric ratio as the horizontal axis. In the diagram, the solid circles indicate the experiments in which the spikes were observed. The transparent circles, on the other hand, indicate the experiments that did not produce the pressure spikes. For each circle, the time of its inception (the first pressure spike or just the origin of the observable pressurization) is also described.

Table 4.2 Summary data from the experiments

Water injection pressure (bar)	Initial water to liquid nitrogen volumetric ratio	Observable spikes	Spike inception or pressurization inception (ms)	$\left(\frac{dp}{dt}\right)_{max}$ (bar/s)
2	0.05	-	-	0.26
2	0.10	-	-	0.21
3	0.05	✓	396	25.0
3	0.10	-	1010	2.89
3	0.15	-	1556	5.70
3	0.20	-	2701	1.26
4	0.05	✓	218	6.47
4	0.10	✓	442	23.6
4	0.15	✓	656	24.8
4	0.20	✓	921	16.1

From the proposed diagram of "Interaction Zone," it can be seen that the experiments with the energetic pressurization process all located in the upper part of the diagram. In addition, their inception times of pressurization are also much faster than those in the experiments located in the lower part.

The rate in which the pressure increased for the spike or the pressurization in each experiment is indicated in the diagram, as shown in Fig. 4.15. It is also observed that all but one of the experiments locate in the top part of the diagram have the relatively much higher pressurization rate compared to the experiments in the lower part.

Based on the diagram of the "Interaction zone," it is concluded that the interaction between the water and the liquid nitrogen can be divided into that of the strong interaction, weak interaction, and without the interaction. As indicated by the diagram, for the experiments with the same water/liquid nitrogen volumetric ratio, the

experiment with the higher water injection pressure is more likely to have the strong interaction. The inception time of the pressurization for the experiment with the strong interaction, which also indicated the beginning of the interaction, is also decreased as the water/liquid nitrogen volumetric ratio gets lower. Similarly, the experiment with the higher water/liquid nitrogen volumetric ratio tended to result in the higher rate of pressurization.

The reason of the interaction pattern as indicated by the "Interaction Zone" diagram was that the water injection pressure and the water/liquid nitrogen volumetric ratio both affected the void fraction. As explained by Meeks et al. [38] that the void fraction could suppress the strong interaction and prevent the process of vapor explosion in a water/molten tin system, the large void fraction in the liquid nitrogen could similarly impede the possibility of the strong interaction with the water and suppress the large pressurization in the system.

From Fig. 4.2(a) and 4.3(a), the water/liquid nitrogen volumetric ratios are low. The large fraction of the water may be injected and came into contact with the liquid nitrogen in a very short period for the mixing of the water and the liquid nitrogen. This short period mixing produced little void fraction. Therefore, the fragmentation of the water droplets and the consequence interactions would be very strong and the large pressurization would be resulted.

From Fig. 4.3 (d), the volume of water used is high. The first portion of the water was injected in the longest period when compared to the same injection pressure with volumetric ratio 0.10 and 0.15. The mixing between water and liquid nitrogen is then longer. Therefore, the mixing along the water jet formed a large void fraction and the consequence interactions would be weakened to 16.1 bar/s when compared to 23.6 and 24.8 bar/s in the case with volumetric ratio 0.10 and 0.15 at the same injection pressure.

It should be noted that more than one pressure spike could be observed in various experiments. This was possible if there were many repetitive strong interactions between the water and the liquid nitrogen. The injection of the water that resulted in a group of the water lumps that sub-sequently interacted with liquid

nitrogen was one of the possible scenarios. One of the other possibilities was the result of the propagation stage of vapor explosion where the high pressure pulse caused by the fragmentation of a lump of water and its strong interaction with the liquid nitrogen triggered the fragmentation of the other lumps of water and initiated their interactions with the liquid nitrogen.

4.3.2 Ice Debris

The presence of the ice debris in the chamber observed after each experiment had been concluded was studied. It was found that the ice debris for the experiments where the pressure spikes were observed or for the experiments that located in the strong interaction zone as indicated by Fig. 4.14 and 4.15 were partially at the bottom of the chamber. A fraction of the fine debris was found dispersing at the wall on the upper part of the chamber. The ice debris found at the bottom of the chamber tended to be powder liked. The larger pieces of the ice debris were jagged and sharp-edged. Some of them even looked like the frozen bubbles that were broken. For comparison, it was observed that the experiment with the water injection of 4 bar and the water/liquid nitrogen volume ratio of 0.15 had more dispersed ice on the wall than the other experiments conducted with the same injection pressure but with lower volume ratio. In the last test, the water traces at the wall on the upper part of the chamber were observed. This was because the duration of the chamber pressure release after the experiment was too long and the dispersed ice was already melted.

For the experiments that showed the weak pressurization, the ice debris was observed to coalesce together into a rather big lump. Its surface was smooth and with very little sharp edged. Only a small fraction of the debris was found dispersed on the wall of the chamber.

Based on this information, it was postulated that the jagged and sharp edged shape of the debris was the result of the strong interaction between the water and the liquid nitrogen. The frozen broken bubble shaped debris suggested that there was the vapor trapped inside the water droplet that expanded and broke out. It was possible that this was possibly the normal air that de-dissolved from the water as it was frozen. However, it was argued that such process should have produced the very fine or the

sponge-like debris and not the relative much larger bubbles that were observed. For this reason, the model of jet penetration and entrapment proposed by Kim et al. [29] might better explain this result.

4.3.3 Pressure Wave Propagation and the Characteristic Sound Speed

In each experiment, the pressure wave would originate from the lower part of the interaction chamber and travel up to the upper part. For this phenomenon, the issue of interest was the propagation velocity of the pressure wave. In general, a pressure profile as obtained was supposedly composed of three separate effects. The first effect was the result from the fact that the liquid nitrogen initially filled into the chamber experienced the slow heating from the wall of the chamber. This gave rise to the pressure in the system even before the water was injected. The initial difference in pressure levels measured by transducer PT1 and PT2 was the evidence of this effect. The second effect was due to the initial mixing of the injected water and the liquid nitrogen. This was observed as the relatively slow rising in pressure just before the first pressure spike was observed. The third effect, the effect that was the cause of the pressure wave, was the effect of the strong interaction between the water and the liquid nitrogen.

Two cases at volumetric ratio 0.05 and 3 or 4 bar(g) injection pressure are considered. Fig. 4.2(a) and 4.3(a) show that the pressure spikes detected by two pressure transducers PT1 and PT2 start increasing almost at the same time. While three cases at 4 bar(g) injection pressure but with volumetric ratio 0.10, 0.15 and 0.20 show the pressure spikes with delay.

The experiment at 4 bar(g) injection pressure and the water/liquid nitrogen volumetric ratio of 0.10 was selected for the demonstration purpose. The pressure profile obtained from this experiment was modified in order to take out the possible effects of the heating wall and the initial mixing. The result of the modification was as shown in Fig.4.16.

To calculate the propagation velocity, it was assumed that the first spikes observed by the transducers were from the same event. The information from the

modified profile necessary for the calculation of the propagation velocity was given in Table 4.3. With the distance of 0.695 meters between transducer PT1 and PT2 and the time interval between the first spikes from the transducers, the propagation velocity was estimated to be between 50 m/s based on the inception time (point 1 in Fig. 4.16) to 22 m/s based on the time of the peak (point 2 in Fig. 4.16).

The magnitudes of the spikes were also considered. It was observed that the magnitude of the delay spike, the spike measured by transducer PT2 at the top of chamber, was greater than that of the spike from the same signal that was detected by transducer PT1 near the bottom. Such characteristic suggested that this was possibly the result of the propagation stage of the vapor explosion [11].

Table 4.3 Spike inception, time at peak and peak pressure appeared at PT1 and PT2

	PT1	PT2	Delay time
Spike inception (ms)	442	456	14
Time at peak (ms)	461	493	32
Peak pressure (bar)	0.4	0.58	-

4.3.4 Sound Speed

To consider if the obtained propagation velocity was reasonable, the actual sound speed in the water/liquid nitrogen mixture was estimated. With the assumption that the water fraction was very low compared with the liquid nitrogen fraction, the model for the two-phase homogeneous flow of the liquid/vapor nitrogen was applied. The speed of sound in the mixture was expressed by Wallis [39] as

$$\frac{1}{c^2} = \left[\alpha\rho_2 + (1-\alpha)\rho_1\right]\left[\frac{\alpha}{\rho_2 c_2^2} + \frac{1-\alpha}{\rho_1 c_1^2}\right]$$

For the above relation, the parameters are defined as:

c is the speed of sound of the homogeneous mixture
α is the void fraction
ρ_1 is the density of the liquid phase
c_1 is the speed of sound of the liquid phase
ρ_2 is the density of the vapor phase
c_2 is the speed of sound of the vapor phase

The sound speed as given above was plotted against the void fraction using the data for the liquid and the vapor nitrogen at one bar as shown in Fig. 4.17(a). It can be seen that the sound speed of the mixture decreases very sharply with the void fraction from that of the single phase, liquid or vapor. From this graph, it is estimated that the sound speed in the liquid/vapor nitrogen mixture is 26.2 m/s at the void fraction of 0.5 and would still be under 50 m/s for the void fraction between 0.1-0.9. The sound speed was again plotted at 2 bar as shown in Fig. 4.17(b). It also shows that the sound speed in the mixture for the void fraction between 0.1-0.9 is less than the propagation velocity of 50 m/s.

Based on the above calculation, it was concluded that the propagation velocities of 22 m/s and 50 m/s were possible. The obtained velocities were also reasonable considering that if the spike inception occurred in the mostly liquid nitrogen, the sound speed would be faster than that calculated for the peak where the interaction already vaporized much of the liquid nitrogen.

4.3.5 Comparison with the high temperature vapor explosion

From the results obtained from the experiments and their analyses, the appearance of the pressure spikes, the ice debris, the pressure wave propagation, the magnitude of the propagated pressure wave, and the comparison between the wave velocity to the predicted characteristic speed of sound in the mixture were found to be comparable and similar to those in the high temperature vapor explosion as explained in the reference [11] in Chapter 2. This suggested that the low temperature vapor explosion was fundamentally similar to that at the high temperature and that the results obtained with the study at the low temperature may be applicable to that at the high temperature.

However, since there were only two pressure transducers in the system and since the distance between them was not very far, the inaccuracy of the measurement could give the very misleading result. Therefore, more data obtained

with better instruments were required for this consideration in order to obtain the accurate results.

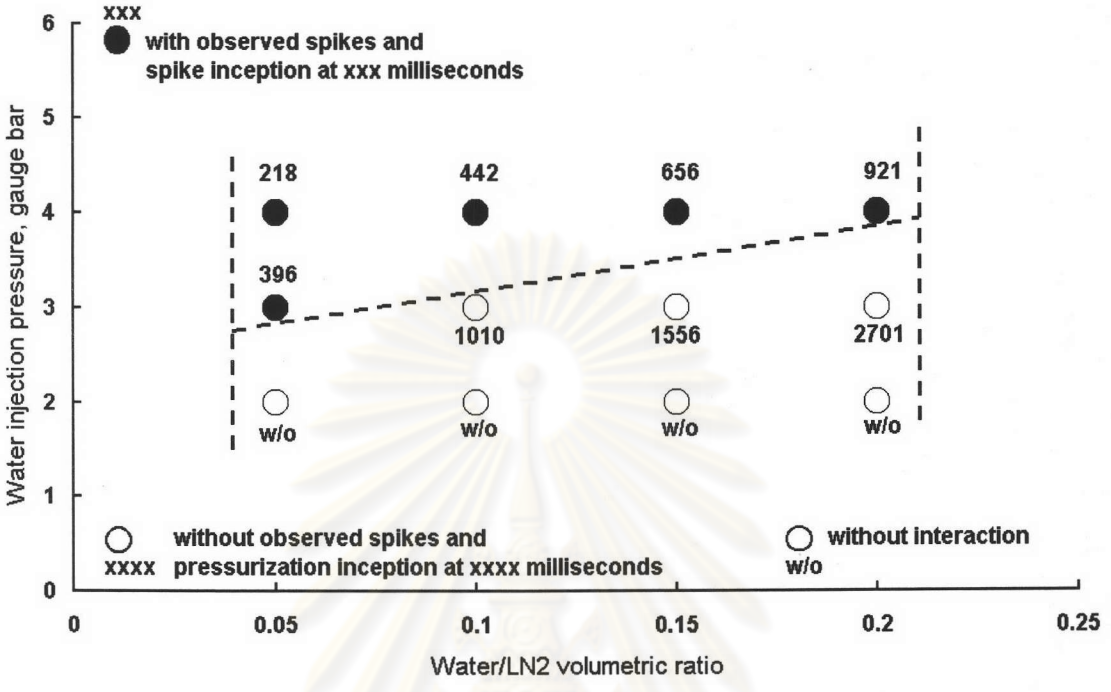

Fig. 4.14 "Interaction Zone" and time of inceptions

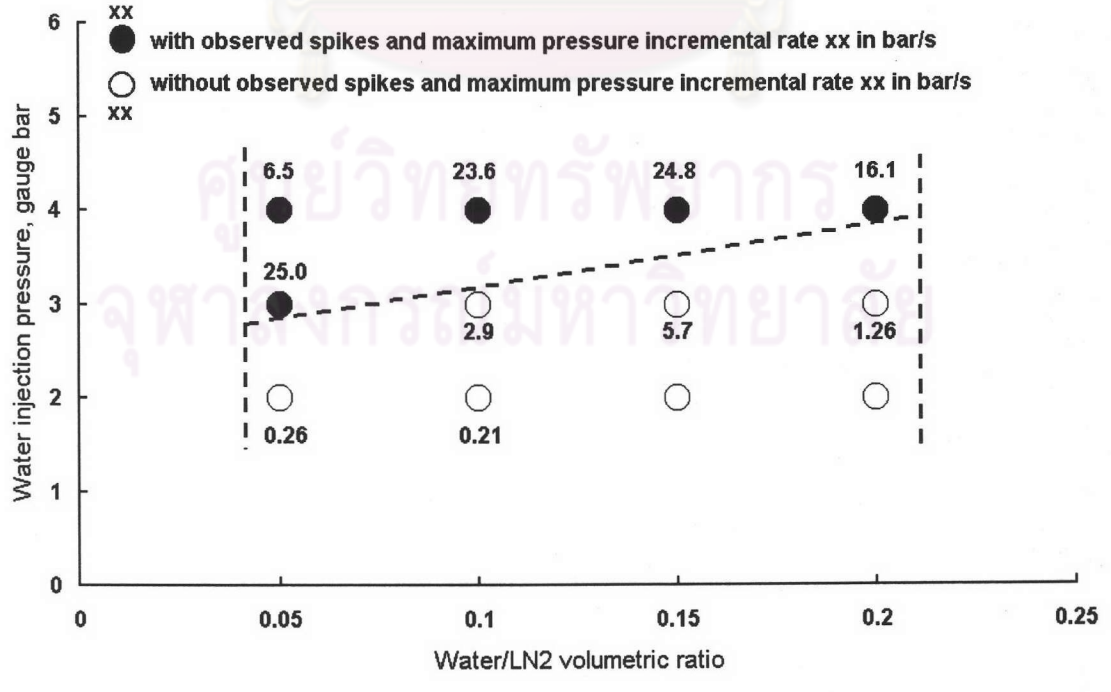

Fig. 4.15 "Interaction Zone" and pressurization rate

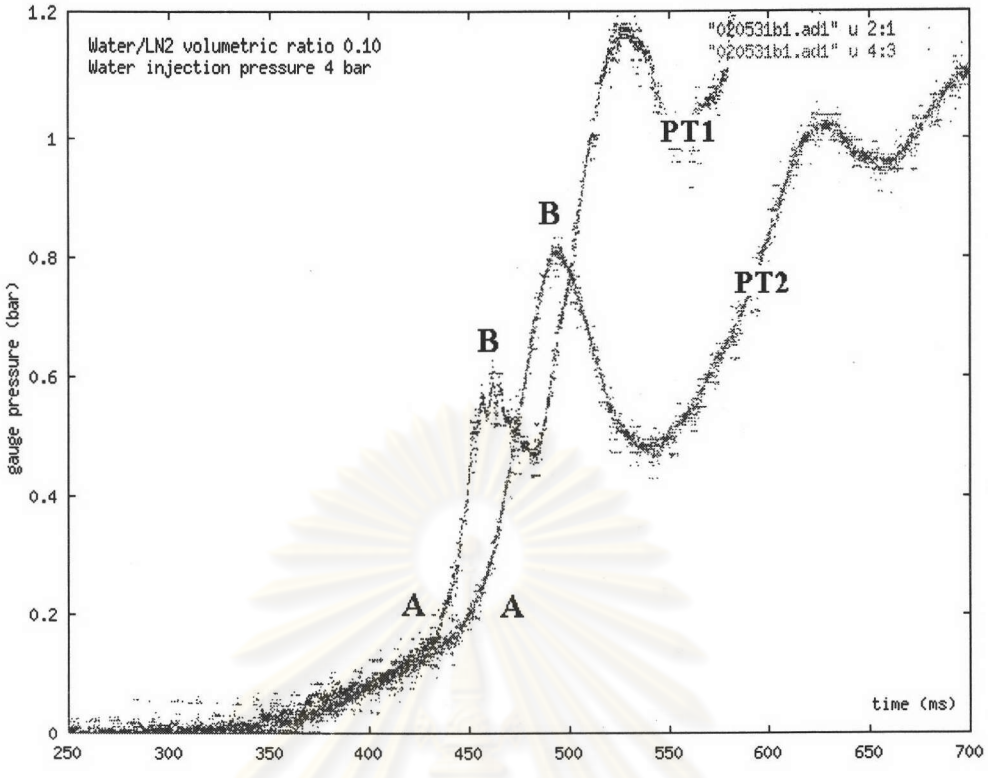

(a) subtract the effect of the heating wall

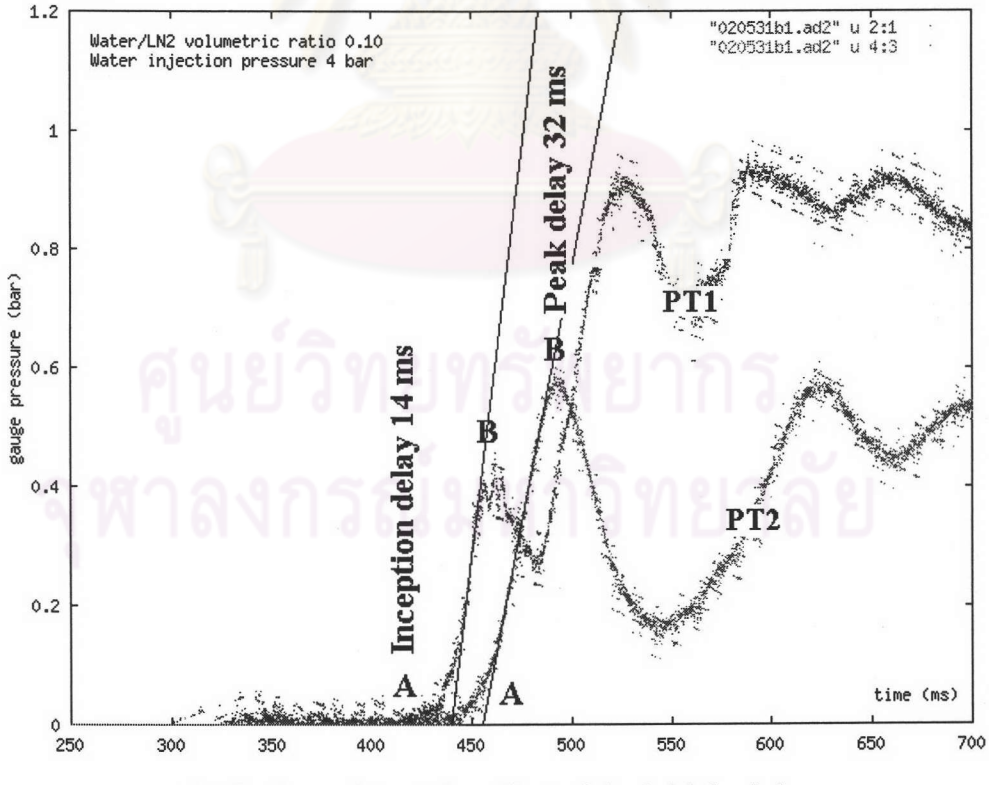

(b) further subtract the effect of the initial mixing

Fig. 4.16 Modified profiles of the experiment with 4 bar water injection pressure and the water/liquid nitrogen volumetric ratio of 0.10

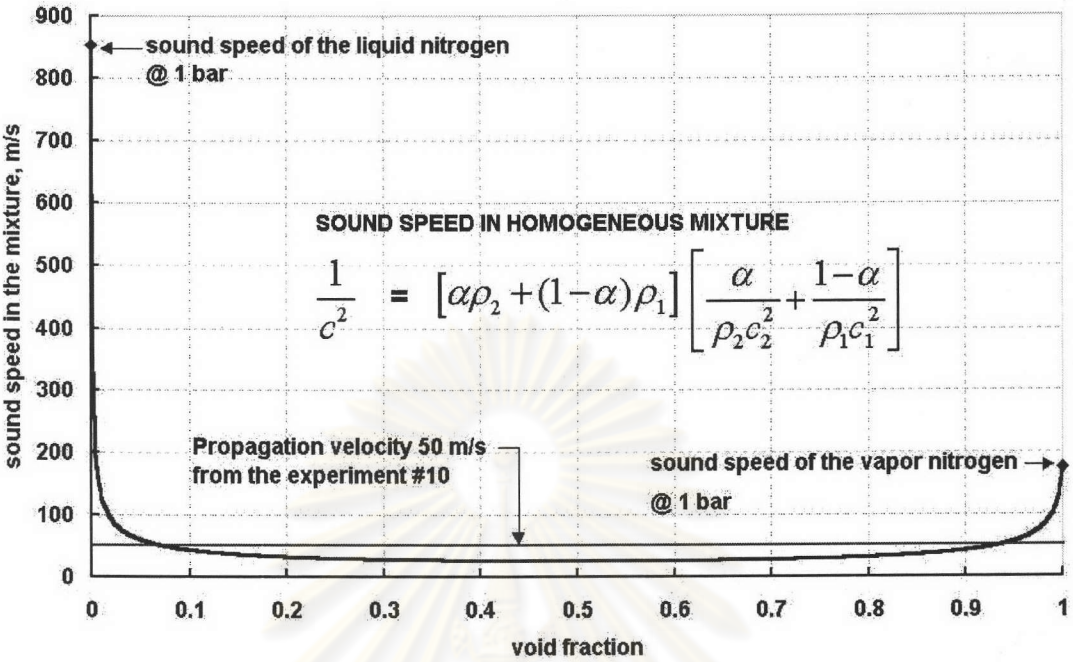

(a) at 1 bar

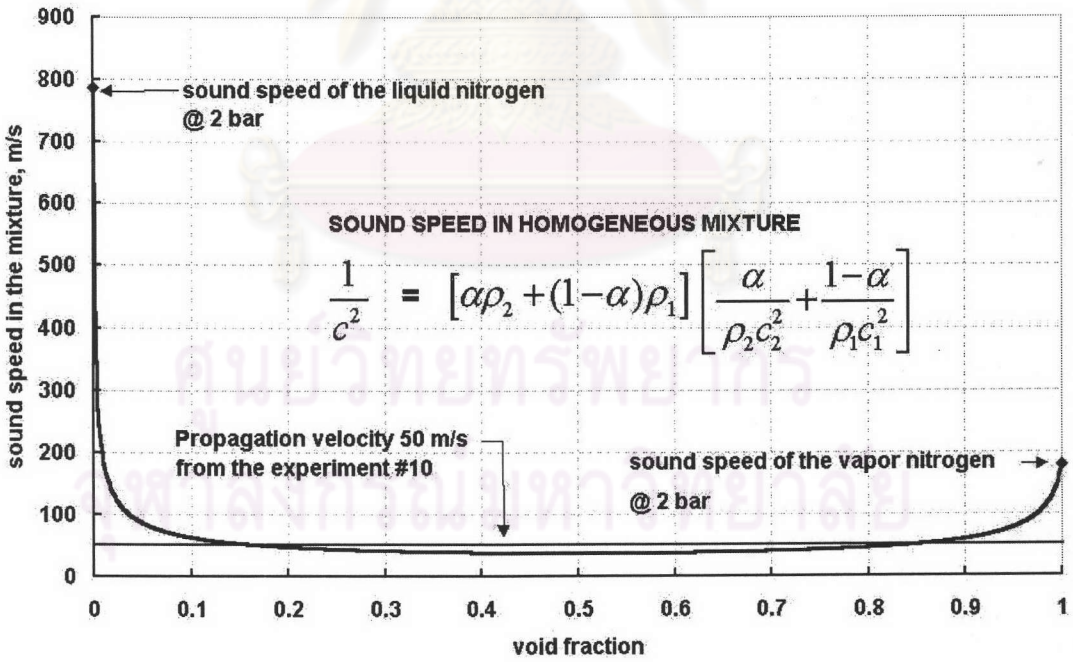

(b) at 2 bar

Fig. 4.17 Sound speed in the liquid/vapor nitrogen mixture